agronomy

MDPI

Communication

Modeling Soil Water Content and Crop-Growth Metrics in a Wheat Field in the North China Plain Using RZWQM2

Kun Du [1,2,3], Yunfeng Qiao [1,2,3,*], Qiuying Zhang [4], Fadong Li [1,2,3], Qi Li [4], Shanbao Liu [1,2,3] and Chao Tian [1,2,3]

1 Key Laboratory of Ecosystem Network Observation and Modeling, Institute of Geographic Sciences and Natural Resources Research, Chinese Academy of Sciences, Beijing 100101, China; duk.17b@igsnrr.ac.cn (K.D.); lifadong@igsnrr.ac.cn (F.L.); liusb.19b@igsnrr.ac.cn (S.L.); tianc@igsnrr.ac.cn (C.T.)
2 Shandong Yucheng Agro-Ecosystem National Observation and Research Station, Ministry of Science and Technology, Yucheng 251200, China
3 College of Resource and Environment, University of Chinese Academy of Sciences, Beijing 100049, China
4 Chinese Research Academy of Environment Sciences, Beijing 100012, China; zhangqy@craes.org.cn (Q.Z.); liqiyr@stu.shzu.edu.cn (Q.L.)
* Correspondence: qiaoyf@igsnrr.ac.cn

Abstract: Soil water content (SWC) is an important factor restricting crop growth and yield in cropland ecosystems. The observation and simulation of soil moisture contribute greatly to improving water-use efficiency and crop yield. This study was conducted at the Shandong Yucheng Agro-ecosystem National Observation and Research Station in the North China Plain. The study period was across the winter wheat (*Triticum aestivum* L.) growth stages from 2017 to 2019. A cosmic-ray neutron probe was used to monitor the continuous daily SWC. Furthermore, the crop leaf area index (LAI), yield, and aboveground biomass of winter wheat were determined. The root zone quality model 2 (RZWQM2) was used to simulate and validate the SWC, crop LAI, yield, and aboveground biomass. The results showed that the simulation errors of SWC were minute across the wheat growth stages and mature stages in 2017–2019. The root mean square error (RMSE) and relative root mean square error (RRMSE) of the SWC simulation at the jointing stage of winter wheat were 0.0296 and 0.1605 in 2017–2018, and 0.0265 and 0.1480 in 2018–2019, respectively. During the rain-affected days, the RMSE (0.0253) and RRMSE (0.0980) for 2017–2018 were significantly lower than those of 2018–2019 (0.0301 and 0.1458, respectively), indicating that rain events decreased the model accuracy in the dry years compared to the wet years. The simulated LAIs were significantly higher than the measured values. The simulated yield value of winter wheat was 5.61% lower and 3.92% higher than the measured yield in 2017–2018 and in 2018–2019, respectively. The simulated value of aboveground biomass was significantly (45.48%) lower than the measured value in 2017–2018. This study showed that, compared with the dry and cold wheat growth period of 2018–2019, the higher precipitation and temperature in 2017–2018 led to a poorer simulation of SWC and crop-growth components. This study indicated that annual abnormal rainfall and temperature had a significant influence on the simulation of SWC and wheat growth, especially under intensive climate-change stress conditions.

Keywords: soil water content; yield; winter wheat; RZWQM2; North China Plain

Citation: Du, K.; Qiao, Y.; Zhang, Q.; Li, F.; Li, Q.; Liu, S.; Tian, C. Modeling Soil Water Content and Crop-Growth Metrics in a Wheat Field in the North China Plain Using RZWQM2. *Agronomy* **2021**, *11*, 1245. https://doi.org/10.3390/agronomy11061245

Received: 26 May 2021
Accepted: 17 June 2021
Published: 19 June 2021

1. Introduction

Soil water content (SWC) is a critical factor influencing soil restoration and plant growth in agricultural ecosystems [1–3], and it has a significant effect on field grain yield by affecting root and leaf growth, and soil microbial activities in croplands [4–7]. Many previous studies monitored cropland SWC at various scales (local to regional) using different methods [3,5,8–13]. The cosmic-ray neutron probe (CRNP) is a reliable method for automatically measuring mean SWC at the hectometer scale without disturbing the soil. In recent years, CRNP was evaluated and successfully applied in various ecosystems [14–20], but its application in croplands under altered weather conditions is insufficiently studied.

The root zone quality model (RZWQM) is an effective and widely used method for evaluating agricultural water resources and crop growth [21,22]. Ma et al. [5] used 26 years of data to evaluate corn and soybean yield, along with water, in a tile-drained field using the RZWQM2 model. Saseendran et al. [23] and Ma et al. [24] suggested that higher soil-water deficit caused lower simulated values of crop LAI and yield. It was reported that the long-term precipitation pattern had a significant influence on crop simulation due to various annual SWC conditions [25]. Therefore, it is critical to simulate SWC under different annual environmental conditions (i.e., precipitation and air temperature), especially under drought and wet conditions.

It has been reported that global climate changes have increased in magnitude of extreme droughts and floods that have occurred worldwide [26]. The altered weather conditions significantly influence SWC and cropland growth components. Sima et al. [27] and Hu et al. [2] suggested that higher supplementary water increased the simulation errors for SWC and crop biomass, and the simulation errors were influenced by the background soil water condition. Therefore, it is necessary to monitor and simulate the response of SWC, and crop growth and grain yield to climate change. The North China Plain (NCP) covers 1.445 million km^2 and is intensively cultivated. Therefore, we conducted an experiment to measure and simulate SWC and crop-growth components for a winter wheat field in the NCP. The objectives of this study were: (1) to simulate SWC and valuate the influence of rainfall under various weather conditions; and (2) to simulate crop-growth components under annual environment conditions in a wheat field in the NCP. The hypotheses of this study are as follows: (1) various annual weather conditions and rain events influence the simulation accuracy of SWC; (2) simulation of crop-growth components is affected by mean soil water during wheat growth stages.

2. Materials and Methods

2.1. Site Description

This study was conducted at the Shandong Yucheng Agro-ecosystem National Observation and Research Station, Ministry of Science and Technology, located in the NCP (36°50′ N, 116°34′ E). The mean annual temperature and precipitation are 13.3 °C and 559.8 mm, respectively. More than 70% of the total annual precipitation occurs from June to September. The annual evaporation ranges from 900 to 1400 mm (1980–2015) [28,29]. The soil type is a calcaric Fluvisol, and the texture of the surface soil is silt loam (sand, 12%; silt, 66%; clay, 22%). In the top 20 cm of the soil layer, the mean pH (soil: water, 1:5) was 8.3, total organic content was 12.6 g kg^{-1}, total N was 0.89 g kg^{-1}, total P was 2.11 g kg^{-1}, and total K was 21.4 g kg^{-1} [30,31].

The mean air temperature was 8.77 °C, and the cumulative rainfall was 408.2 mm during the wheat growth stage in 2017–2018; it was 8.34 °C and 120.2 mm during the wheat growth stage in 2018–2019 (Figure 1).

2.2. Field Management and Experiment Design

In the NCP, the main local crop rotation is winter wheat–summer maize. As in the experimental region, the winter wheat seeds were mechanically sowed after plowing with residual straw return in mid-October. A 100 mm irrigation (local groundwater) and nitrogen fertilization were carried out in late March of the following year, and the second 100 mm was applied in mid-May. However, the second irrigation in 2017–2018 was not applied due to excess precipitation in April 2018. Wheat was harvested in early June. The other farmland management measures, such as pesticide spraying and weeding, were conducted according to the local management.

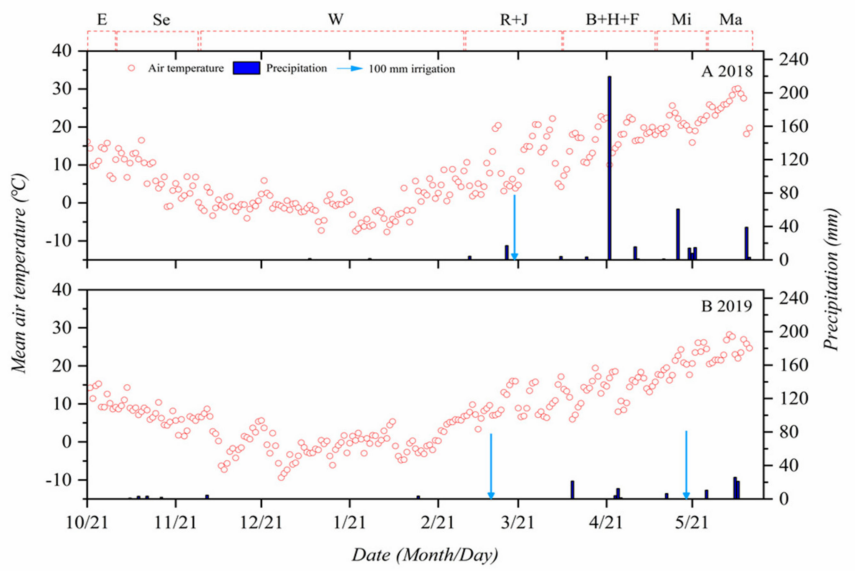

Figure 1. Daily air temperature and precipitation during the wheat growth stages in 2017–2019. Red dash line is used to mark the wheat growth stages: E, emergency; Se, seedling; W, wintering; R + J: Returning green and Jointing; B + H + F: Booting, heading and flowering; Mi: Milking; Ma: Mature.

2.3. SWC and Crop Biomass Monitoring and Measurement

In early September 2017, a CRNP (CRS100, Prebo Technology Co., Ltd., Beijing, China) was installed in the comprehensive observation field at the Yucheng experiment station. This CRNP was installed at over 5 m distance from other instruments to reduce ray interference. The neutron instrument was mainly composed of a neutron-detector instrument, a data acquisition and program control box, DC power supply system, and support frame. The neutron detector was placed vertically 0.50 m above the ground, and the cumulative number of neutrons was output every hour. The source area radius and detection depth formula used were described by the previous study [32]. After calculation, the soil depth detected by the neutron instrument in this study was 0.29 m. Because the cosmic-ray neutron instrument operates under different air pressure in different locations, it was necessary to convert and calibrate the neutron number measured by the neutron instrument [15].

$$N = N_{raw} \times \exp\{\beta \times (p - p_0)\} \quad (1)$$

where N is the number of fast neutrons after correction, N_{raw} is the original number of fast neutrons measured, β is a constant (0.0077), p is the real-time pressure value (kPa) at a given time, and p_0 is the local theoretical pressure value (kPa).

Taking the CRNP as the center of the monitoring area in the station, we radially divided the resource area into 60° sectors, and we arranged three concentric sampling rings at 20 m, 75 m, and 150 m distance from the center on each of the six radial lines, producing 18 sampling points. At each sample point, we collected six soil samples between 0 and 30 cm (one sample at each 5 cm interval) using the ring knife method. The soil samples were immediately returned to the laboratory for drying to a constant weight over 72 h, after which the mean soil volumetric water content of each point was obtained. The mean SWC value of 18 sampling points was used to represent the soil volumetric water content of the contribution area at this station. We used the mean SWC as the measured θ to calculate the standard fast neutrons N_0 using the following equation [15]:

$$\theta = \frac{a_0}{(N/N_0) - a_1} - a_2 \quad (2)$$

where θ is the measured soil volumetric water content ($cm^3\ cm^{-3}$); N_0 is the number of fast neutrons under dry conditions after calibration; N is the number of neutrons measured

during the sampling hours; and a_0, a_1, and a_2 are constants 0.0808, 0.372, and 0.115, respectively. After obtaining N_0, the SWC was measured using the calculated N.

The main field plots in the experimental station were divided into six, and the LAI and aboveground biomass of winter wheat at the station were measured during the wheat harvest period, and plots (1 m × 1 m, six replicates) were randomly selected. The aboveground biomass (Mg ha^{-1}) and yield (Mg ha^{-1}) of winter wheat samples were calculated using the oven-drying method. Meteorological parameters including daily maximum, minimum, and mean air temperature (°C), relative humidity (%), wind speed (m/s), cumulative daily solar radiation, and rainfall (mm) were automatically observed at this station as the driving variables of the simulation model.

2.4. Simulation and Validation of SWC and Crop Biomass

The RZWQM2 model was used to simulate the soil moisture, LAI, aboveground biomass, and yield of winter-wheat in the two wheat seasons of 2017–2019. The detailed information of the RZWQM2 could refer the study of Ahuja et al. [33]. The simulation of SWC used the measured air temperature, air humidity, wind speed, rainfall and soil physical parameters in the module of SWC physical transfer process, and soil nutrients were input into the related nutrients module [30,31,33,34]. The Brooks Corey equation was used to describe the soil moisture characteristic curve, and the Richards equation was used to measured soil water redistribution between soil layers [33,34]. We input farmland management parameters, for example, irrigation, fertilization, wedding and the default winter wheat genetic parameters into crop growth and cropland management modules for the simulation of crop growth [33,35]. We used the SWC data during the wheat growth stages in 2017–2018 to calibrate the RZWQM2, and we used the SWC data in 2018–2019 to validate this model. The simulation evaluation index uses the root mean square error (RMSE) and relative root mean square error (RRMSE), which are expressed as follows:

$$RMSE = \sqrt{\frac{1}{n}\sum_{i=1}^{n}(Si - Oi)^2} \quad (3)$$

$$RRMSE = \frac{R_{MSE}}{\overline{O}} \times 100\% \quad (4)$$

where RMSE is the root mean square error and RRMSE is the relative root mean square error. The smaller the error, the better is the simulation accuracy. Si is the simulated SWC value numbered i, Oi is the measured SWC value numbered i, $\bar{O}$ is the arithmetic mean of all observations, and n is the number of measured values.

3. Results

The measured average daily SWC of the 2017–2018 winter wheat season was 0.184 cm^3 cm^{-3}, which was significantly higher than that of the 2018–2019 wheat season, 0.179 cm^3 cm^{-3} (Figure 2). The simulated soil moisture results during the winter wheat growth period showed that in the 2017–2018 winter wheat season, the quality of soil moisture simulation was best at the jointing stage, with RMSE and RRMSE of 0.0129 and 0.0569, respectively (Table 1). The RRMSE at the emergence stage was 0.2866, and the simulation accuracy was poor. In the 2018–2019 wheat season, the simulation of SWC during the milking stage was the worst, and the simulation at the jointing and mature stages were the best, with RRMSE values of 0.1082 and 0.0959, respectively. Overall, the simulation errors of the winter wheat season in 2018–2019 were lower than that in 2017–2018 (Figure 2). Rainfall in the 2 study years had a certain impact on the simulation error. For the simulation error during rain-affected days in 2017–2018, the RMSE and RRMSE were 0.0253 and 0.0980, respectively, which was significantly lower than those of 0.0301 and 0.1458 in 2018–2019 (Figure 2).

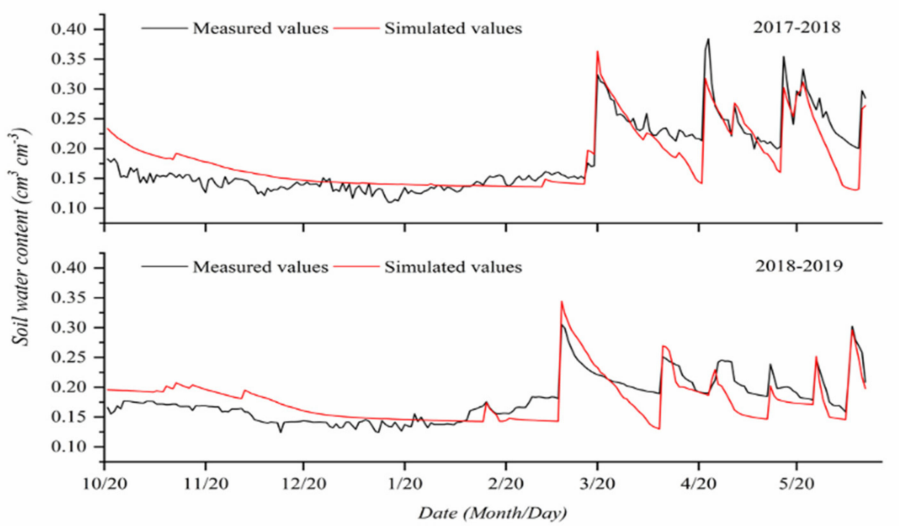

Figure 2. Measured and simulated values of soil water content during wheat growth stages in 2017–2019.

Table 1. Simulation errors of soil water content during wheat growth stages in 2017–2019.

Growth Stages	2017–2018		2018–2019	
	RMSE	RRMSE	RMSE	RRMSE
Emergency	0.0479	0.2866	0.0266	0.1569
Wintering	0.0147	0.1065	0.0229	0.1508
Jointing	0.0148	0.0651	0.0241	0.1082
B + H + F	0.0434	0.1775	0.0307	0.1462
Milking	0.0196	0.0866	0.0434	0.2062
Mature	0.0483	0.1829	0.0188	0.0959

B + H + F: booting, heading and flowering stages.

The simulation of LAI was not significant ($p > 0.05$) (Table 2). For the 2 seasons of 2017 to 2019, the measured grain yield was 5.88 and 6.12 Mg ha^{-1}, respectively (Table 2). The simulated grain yield was significantly below the actual measured value by 5.61% in 2017–2018, and above in 2018–2019 by 3.92% (Table 2). Although the measured aboveground biomass of 2018–2019 exceeded that of the preceding year, the simulation error was lower, being just 14.79% compared to 45.48% in 2017–18 (Table 2).

Table 2. Measured and simulated values of wheat leaf area index (cm^2 cm^{-2}), grain yield (Mg ha^{-1}) and aboveground biomass (Mg ha^{-1}) during wheat growth stages in 2017–2019.

Study Period	Item	Leaf Area Index	Grain Yield	Aboveground Biomass
2017–2018	Measured values	1.91	5.88	9.11
	Simulated values	1.65	5.55	13.26
	RMSE	0.42	3.40	4.14
	RRMSE	0.2566	0.0577	0.4548
2018–2019	Measured values	2.30	6.12	11.19
	Simulated values	2.04	6.36	12.85
	RMSE	0.46	2.39	1.67
	RRMSE	0.2257	0.0390	0.1479

4. Discussion

The simulation errors of SWC with RZWQM2 were small in this study (Table 1), in line with the results reported earlier [2,36,37]. Kersebaum et al. [38] suggested that the

RMSE of SWC was less than 0.05 cm^3 cm^{-3}, but greater than 0.02 cm^3 cm^{-3}. In this study, the dynamic simulation of SWC was presented with a variant of the growth period, and the simulation accuracy was relatively higher at the jointing and mature stages (Figure 2, Table 1), supporting our first proposed hypothesis. This could be explained by the fact that winter wheat begins to enter the high-growth stages in mid-March, when the demand for soil water is higher, and SWC was relatively stable at the mature stage. Furthermore, the increased rainfall from April to June resulted in higher errors in the SWC simulation during those two months in 2017–2018 (Figure 2), similar to the study conducted by Xu et al. [39].

In this study, the simulation for SWC at 0–30 cm soil depth varied after rainfall (Figure 2), and rain events resulted in a poor simulation, as some previous studies suggested [39,40]. These results supported the first proposed hypothesis. A lower SWC simulation accuracy was observed during the wheat growth stage in 2017–2018 than in 2018–2019 (Figure 2) due to higher rainfall resulting in greater SWC variation in that year (Figure 1). Sima et al. [27] found that a higher irrigation quantity increased SWC simulation errors compared to lower irrigation levels. By contrast, the SWC simulation accuracy across the rain-affected days was lower during 2018–2019 than that during 2017–2018 (Figure 2). This resulted from drier soil during the wheat season in 2018–2019, especially in April to June, which was more sensitive to precipitation, leading to complicated SWC variation and poor simulation. In this study, the first 100 mm irrigation was applied on March (Figure 1), and the daily simulation errors of SWC immediately increased after irrigation and fast return to that before irrigation within 5 days in 2017–2018 (Figure 2). By contrast, the simulation accuracy had no significant response to the first irrigation in 2018–2019 (Figure 2). This could be explained by the fact that the background SWC levels were different, and the relatively wetter soil with higher SWC was not sensitive to soil water addition in early March in 2018–2019, leading to various influences of irrigation on SWC simulation.

It was reported that heavy drought resulted in lower simulated LAI and grain yield when compared with measured values, and led to poor simulation [23,24]. In this study, the simulation of LAI was not significant (Table 2), even though we found the simulated SWC was in line with measured SWC, contrasting with our second hypothesis. Furthermore, Pauwels et al. [41] suggested that the assimilation of SWC had no influence on improving crop LAI simulation. However, some studies conducted that measured SWC enhanced grain yield prediction, while the simulation errors varied with models, climate styles and study years [42,43]. In our study, the simulated grain yield across the 2 study years agreed well with the measured values in this study (Table 2), similar to the study conducted by Sima et al. [27] and Xu et al. [39], by using RZWQM2. This study highlighted that the wheat yield simulation was in an effective range under different annual rainfall and temperature conditions. By contrast, the simulation of crop biomass was poorer in 2017–2018 (Table 2), resulting from excessive rainfall and subsequent wheat flattening after the heavy precipitation occurred on April 9 (Figure 1).

Soil water content is an important constraint limiting crop growth in arid and semi-arid areas, and the simulation of SWC is of great significance for the timely understanding of crop growth and farmland management [1,18]. In this study, the influence of rainfall on simulation errors of SWC was extremely significant. Furthermore, increasing variation in meteorological conditions, such as rainfall and temperature fluctuations, are expected owing to global climate change in the future. Therefore, continuous monitoring of SWC and crop physiological elements under various weather conditions is urgently needed, and it is of great significance for the verification of the model.

Author Contributions: Conceptualization, K.D., Y.Q., F.L., and Q.Z.; methodology, K.D., F.L., and Q.L.; software, K.D. and Q.L.; formal analysis, K.D. and Q.L.; investigation, K.D., S.L., and C.T.; writing—original draft preparation, K.D. and Q.L.; writing—review and editing, F.L. and K.D.; supervision, K.D., Y.Q., and F.L. All authors have read and agreed to the published version of the manuscript.

Funding: This research was funded by the National Key Research and Development Program of China (No. 2016YFC0500101, 2016YFD0800301), and the National Natural Science Foundation of China (No. U1906219, 42007155, U2006212).

Institutional Review Board Statement: Not applicable.

Informed Consent Statement: Not applicable.

Acknowledgments: We would like to thank colleagues at the Yucheng experimental station for experimental support and constructive advice on this manuscript.

Conflicts of Interest: The authors declare no conflict of interest.

References

1. Vereecken, H.; Huisman, J.A.; Franssen, H.J.H.; Brueggemann, N.; Bogena, H.R.; Kollet, S.; Javaux, M.; Van Der Kruk, J.; Vanderbor-ght, J. Soil hydrology: Recent methodological advances, challenges, and perspectives. *Water Resour. Res.* **2015**, *51*, 2616–2633. [CrossRef]
2. Hu, C.; Saseendran, S.A.; Green, T.R.; Ma, L.; Li, X.; Ahuja, L.R. Evaluating nitrogen and water management in a double-cropping system using RZWQM. *Vadose Zone J.* **2006**, *5*, 493–505. [CrossRef]
3. Hammami, Z.; Qureshi, A.S.; Sahli, A.; Gauffreteau, A.; Chamekh, Z.; Ben Azaiez, F.E.; Ayadi, S.; Trifa, Y. Modeling the Effects of Irrigation Water Salinity on Growth, Yield and Water Productivity of Barley in Three Contrasted Environments. *Agronomy* **2020**, *10*, 1459. [CrossRef]
4. Jia, X.; Shao, M.; Wei, X.; Wang, Y. Hillslope scale temporal stability of soil water storage in diverse soil layers. *J. Hydrol.* **2013**, *498*, 254–264. [CrossRef]
5. Ma, L.; Malone, R.W.; Heilman, P.; Karlen, D.L.; Kanwar, R.S.; Cambardella, C.A.; Saseendran, S.A.; Ahuja, L.R. RZWQM simulation of long-term crop production, water and nitrogen balances in Northeast Iowa. *Geoderma* **2007**, *140*, 247–259. [CrossRef]
6. Kim, S.; Meki, M.N.; Kim, S.; Kiniry, J.R. Crop modeling application to improve irrigation efficiency in year-round vegetable production in the texas winter garden region. *Agronomy* **2020**, *10*, 1525. [CrossRef]
7. Song, S.; Zhang, S.; Wang, T.; Meng, J.; Zhou, Y.; Zhang, H. Balancing conservation and development in Winter Olympic construc-tion: Evidence from a multi-scale ecological suitability assessment. *Sci. Rep.* **2018**, *8*, 14083. [CrossRef]
8. Chen, X.; Qi, Z.; Gui, D.; Gu, Z.; Ma, L.; Zeng, F.; Li, L.; Sima, M.W. A Model-Based Real-Time Decision Support System for Irrigation Scheduling to Improve Water Productivity. *Agronomy* **2019**, *9*, 686. [CrossRef]
9. Fang, Q.; Ma, L.; Harmel, R.D.; Yu, Q.; Sima, M.W.; Bartling, P.N.S.; Malone, R.W.; Nolan, B.T.; Doherty, J. Uncertainty of ceres-maize calibration under different irrigation strategies using PEST optimization algorithm. *Agronomy* **2019**, *9*, 241. [CrossRef]
10. Zhu, X.; Shao, M.; Zeng, C.; Jia, X.; Huang, L.; Zhang, Y.; Zhu, J. Application of cosmic-ray neutron sensing to monitor soil water content in an alpine meadow ecosystem on the northern Tibetan Plateau. *J. Hydrol.* **2016**, *536*, 247–254. [CrossRef]
11. Zeng, J.; Li, Z.; Chen, Q.; Bi, H. Method for Soil Moisture and Surface Temperature Estimation in the Tibetan Plateau Using Spaceborne Radiometer Observations. *IEEE Geosci. Remote. Sens. Lett.* **2014**, *12*, 97–101. [CrossRef]
12. Phogat, V.; Mahadevan, M.; Skewes, M.; Cox, J.W. Modelling soil water and salt dynamics under pulsed and continuous surface drip irrigation of almond and implications of system design. *Irrig. Sci.* **2012**, *30*, 315–333. [CrossRef]
13. Tian, S.; Tregoning, P.; Renzullo, L.J.; Van Dijk, A.I.J.M.; Walker, J.P.; Pauwels, V.R.N.; Allgeyer, S. Improved water balance com-ponent estimates through joint assimilation of GRACE water storage and SMOS soil moisture retrievals. *Water Resour. Res.* **2017**, *53*, 1820–1840. [CrossRef]
14. Pinnington, E.; Amezcua, J.; Cooper, E.; Dadson, S.; Ellis, R.; Peng, J.; Robinson, E.; Morrison, R.; Osborne, S.; Quaife, T. Improving soil moisture prediction of a high-resolution land surface model by parameterising pedotransfer functions through assimilation of SMAP satellite data. *Hydrol. Earth Syst. Sci.* **2021**, *25*, 1617–1641. [CrossRef]
15. Zhu, X.; Shao, M.; Jia, X.; Huang, L.; Zhu, J.; Zhang, Y. Application of temporal stability analysis in depth-scaling estimated soil water content by cosmic-ray neutron probe on the northern Tibetan Plateau. *J. Hydrol.* **2017**, *546*, 299–308. [CrossRef]
16. Baroni, G.; Scheiffele, L.; Schrön, M.; Ingwersen, J.; Oswald, S. Uncertainty, sensitivity and improvements in soil moisture estimation with cosmic-ray neutron sensing. *J. Hydrol.* **2018**, *564*, 873–887. [CrossRef]
17. Fersch, B.; Francke, T.; Heistermann, M.; Schroen, M.; Doepper, V.; Jakobi, J.; Baroni, G.; Blume, T.; Bogena, H.; Budach, C.; et al. A dense network of cosmic-ray neutron sensors for soil moisture observation in a highly instrumented pre-Alpine headwater catchment in Germany. *Earth Syst. Sci. Data* **2020**, *12*, 2289–2309. [CrossRef]
18. Mwangi, S.; Zeng, Y.; Montzka, C.; Yu, L.; Su, Z. Assimilation of Cosmic-Ray Neutron Counts for the Estimation of Soil Ice Con-tent on the Eastern Tibetan Plateau. *J. Geophys. Res. Atmos.* **2020**, *125*, e2019JD031529. [CrossRef]
19. Scheiffele, L.M.; Baroni, G.; Franz, T.E.; Jakobi, J.; Oswald, S.E. A profile shape correction to reduce the vertical sensitivity of cos-mic-ray neutron sensing of soil moisture. *Vadose Zone J.* **2020**, *19*, e20083. [CrossRef]
20. Duygu, M.B.; Akyurek, Z. Using cosmic-ray neutron probes in validating satellite soil moisture products and land surface models. *Water* **2019**, *11*, 1362. [CrossRef]
21. Kumar, A.; Kanwar, R.S.; Singh, P.; Ahuja, L.R. Evaluation of the root zone water quality model for predicting water and NO3-N movement in an Iowa soil. *Soil Tillage Res.* **1999**, *50*, 223–236. [CrossRef]

22. Liu, C.; Qi, Z.; Gu, Z.; Gui, D.; Zeng, F. Optimizing Irrigation Rates for Cotton Production in an Extremely Arid Area Using RZWQM2-Simulated Water Stress. *Trans. ASABE* **2017**, *60*, 2041–2052. [CrossRef]
23. Saseendran, S.A.; Ma, L.; Malone, R.; Heilman, P.; Ahuja, L.R.; Kanwar, R.S.; Karlen, D.L.; Hoogenboom, G. Simulating, management effects on crop production, tile drainage, and water quality using RZWQM-DSSAT. *Geoderma* **2007**, *140*, 297–309. [CrossRef]
24. Ma, L.W.; Nielsen, D.C.; Ahuja, L.R.; Kiniry, J.R.; Hanson, J.D.; Hoogenboom, G. An evaluation of RZWQM, CROPGRO, and CERES-maize for responses to water stress in the central great plains of the US. In *Agricultural System Models in Field Research and Technology Transfer*; CRC Press: Boca Raton, FL, USA, 2002; pp. 119–148.
25. Bai, X.; Jia, X.; Jia, Y.; Shao, M.; Hu, W. Modeling long-term soil water dynamics in response to land-use change in a semi-arid area. *J. Hydrol.* **2020**, *585*, 124824. [CrossRef]
26. IPCC. Summary for Policymakers. In *Climate Change 2013: The Physical Science Basis. Contribution of Working Group I to the Fifth Assessment Report of the Intergovernmental Panel on Climate Change*; Cambridge University Press: Cambridge, UK, 2013.
27. Sima, M.W.; Fang, Q.X.; Qi, Z.; Yu, Q. Direct assimilation of measured soil water content in Root Zone Water Quality Model calibration for deficit-irrigated maize. *Agron. J.* **2020**, *112*, 844–860. [CrossRef]
28. Zhao, X.; Li, F.; Ai, Z.; Li, J.; Gu, C. Stable isotope evidences for identifying crop water uptake in a typical winter wheat–summer maize rotation field in the North China Plain. *Sci. Total. Environ.* **2018**, *618*, 121–131. [CrossRef]
29. Tu, C.; Li, F. Responses of greenhouse gas fluxes to experimental warming in wheat season under conventional tillage and no-tillage fields. *J. Environ. Sci.* **2017**, *54*, 314–327. [CrossRef] [PubMed]
30. Du, K.; Li, F.; Leng, P.; Li, Z.; Tian, C.; Qiao, Y.; Li, Z. Differential Influence of No-Tillage and Precipitation Pulses on Soil Hetero-trophic and Autotrophic Respiration of Summer Maize in the North China Plain. *Agronomy* **2020**, *10*, 2004. [CrossRef]
31. Du, K.; Li, F.; Qiao, Y.; Leng, P.; Li, Z.; Ge, J.; Yang, G. Influence of no-tillage and precipitation pulse on continuous soil respiration of summer maize affected by soil water in the North China Plain. *Sci. Total. Environ.* **2021**, *766*, 144384. [CrossRef]
32. Franz, T.E.; Zreda, M.; Ferre, T.P.A.; Rosolem, R.; Zweck, C.; Stillman, S.; Zeng, X.; Shuttleworth, W.J. Measurement depth of the cosmic ray soil moisture probe affected by hydrogen from various sources. *Water Resour. Res.* **2012**, *48*, W08515. [CrossRef]
33. Ahuja, L.R.; Rojas, K.W.; Hanson, J.D.; Shaffer, M.J.; Ma, L. *Modeling Management Effects on Water Quality and Crop Production. Root Zone Water Quality Model*; Water Resources Publications, LLC: Littleton, CO, USA, 2000; pp. 372–379.
34. Fang, Q.-X.; Yu, Q.; Wang, J.-L. Simulating Soil Water Dynamics and Its Effects on Crop Yield Using RZWQM- CERES in the North China Plain. *Acta Agron. Sin.* **2009**, *35*, 1122–1130. [CrossRef]
35. Hanson, J.D.; Rojas, K.W.; Shaffer, M.J. Calibrating the Root Zone Water Quality Model. *Agron. J.* **1999**, *91*, 171–177. [CrossRef]
36. Yu, Q.; Saseendran, S.A.; Ma, L.; Flerchinger, G.N.; Green, T.R.; Ahuja, L.R. Modeling a wheat-maize double cropping system in China using two plant growth modules in RZWQM. *Agric. Syst.* **2006**, *89*, 457–477. [CrossRef]
37. Fang, Q.; Ma, L.; Yu, Q.; Malone, R.W.; Saseendran, S.A.; Ahuja, L.R. Modeling Nitrogen and Water Management Effects in a Wheat-Maize Double-Cropping System. *J. Environ. Qual.* **2008**, *37*, 2232–2242. [CrossRef] [PubMed]
38. Kersebaum, K.C.; Hecker, J.-M.; Mirschel, W.; Wegehenkel, M. *Modelling Water and Nutrient dynamics in Soil-Crop systems: A Comparison of Simulation Models Applied on Common Data Sets*; Springer: Dordrecht, The Netherlands, 2007.
39. Xu, J.; Cai, H.; Wang, X.; Ma, C.; Lu, Y.; Ding, Y.; Wang, X.; Chen, H.; Wang, Y.; Saddique, Q. Exploring optimal irrigation and nitrogen fertilization in a winter wheat-summer maize rotation system for improving crop yield and reducing water and nitrogen leaching. *Agric. Water Manag.* **2020**, *228*, 105904. [CrossRef]
40. Han, E.; Merwade, V.; Heathman, G.C. Application of data assimilation with the Root Zone Water Quality Model for soil moisture profile estimation in the upper Cedar Creek, Indiana. *Hydrol. Process.* **2012**, *26*, 1707–1719. [CrossRef]
41. Pauwels, V.R.N.; Verhoest, N.E.C.; De Lannoy, G.J.M.; Guissard, V.; Lucau, C.; Defourny, P. Optimization of a coupled hydrolo-gy-crop growth model through the assimilation of observed soil moisture and leaf area index values using an ensemble Kalman filter. *Water Resour. Res.* **2007**, *43*, W04421. [CrossRef]
42. De Wit, A.M.; Van Diepen, C.A. Crop model data assimilation with the Ensemble Kalman filter for improving regional crop yield forecasts. *Agric. For. Meteorol.* **2007**, *146*, 38–56. [CrossRef]
43. Nearing, G.S.; Crow, W.T.; Thorp, K.R.; Moran, M.S.; Reichle, R.H.; Gupta, H.V. Assimilating remote sensing observations of leaf area index and soil moisture for wheat yield estimates: An observing system simulation experiment. *Water Resour. Res.* **2012**, *48*, W25525. [CrossRef]